Polyvinyltoluene scintillators for relative ion dosimetry: An investigation with Helium, Carbon and Neon beams

D. Broggio, R. Barillon, J.M. Jung, N. Yasuda, T. Yamauchi, H. Kitamura, P. Bischoff

Polyvinyltoluene scintillators for relative ion dosimetry: an investigation with Helium, Carbon and Neon beams.

David Broggio[a], Rémi Barillon[a *], Jean-Marc Jung[a] , Nakahiro Yasuda[b], Tomoya Yamauchi[c] Hisashi Kitamura [b], and Pierre Bischoff [d]

[a] *Institut de Recherches Subatomiques and Université Louis Pasteur, 23 rue du Loess, 67037 Strasbourg, France.*

[b] *National Institute of Radiological Sciences, 4-9-1 Anagawa, Inage, Chiba 263-8555, Japan.*

[c] *Faculty of Maritime Sciences, Kobe University, 5-1-1 Fukaeminami-machi, Kobe 658-0022, Japan*

[d] *Laboratory of Experimental Cancerology and Radiobiology, ULP EA 3430, IRCAD, 1 place de l'Hôpital, 67091, Strasbourg, France*

Abstract

We present a dosimeter prototype, devoted to ion beam dosimetry, tested with Helium, Carbon and Neon ions having an equivalent range in water of 150 mm. A polyvinyltoluene based plastic scintillator is used to convert the deposited energy into scintillation, a measurement probe and a long optical fibre guide the light to a photon counting unit. Using 10-40 µm thick scintillators we show that the dosimeter gain is enough to provide useful measurements, the ion-induced scintillation can be interpreted using a model taking into account the energy deposited by secondary electrons. For a practical purpose it is shown that a linear relationship can be established between the scintillation signal and the relative dose.

Keywords: Scintillation detectors, dosimetry, ion radiation effects, ion-induced scintillation.

[*] Contact author : remi.barillon@ires.in2p3.fr, +33 (0)3 88 10 64 09 (phone) ,+ 33 (0)3 88 10 64 31 (fax)

I. Introduction

Different kinds of radiation are nowadays used in radiation therapy or radiobiological experiments. Since radiobiological effects are always described as a function of the delivered dose the quality of treatments or experiments strongly relies on the accuracy of dose measurements. Several dosimetric techniques are commonly used, either to calibrate the beam or to monitor the dose during irradiation: ionisation chambers, nuclear tracks detectors, semiconductor devices or calorimeters [1-4]. As underlined by Fukumura most of these measurements are relative and only calorimetry enables an absolute dose measurement [1]. Body phantoms can be used to assess the dose in deep organs; as a complementary method complex treatment planning computer codes are used to compute the radiation field in target organs, especially in hadrontherapy where long range ions, crossing several materials, are used.

The lack of compact enough devices, enabling *in vivo* measurements, has motivated the development of dosimeters based on the coupling of scintillators and optical fibres. Most of these small sized dosimeters are devoted to conventional photon therapy, as those presented by Beddar *et al.,* for use in stereotactic radiosurgery [5-6], or by Fontbonne *et al.* for use in brachyterapy [7]. Pain *et al.* have also presented a dosimeter allowing *in vivo* measurements of low dose β emission [8-9]. The potential use of plastic scintillators for the dosimetry in hadrontherapy has only been demonstrated for protons by Torissi [10]. All these authors have already emphasized the usefulness of plastic scintillators whose density makes them water equivalent and thus suitable for direct dose measurement.

We have investigated the use of a plastic scintillator, coupled with an optical fibre associated to a counting electronics, in order to perform dosimetry of ions heavier than the proton. The experiments have been carried out at the HIMAC facility (Heavy Ion Medical Accelerator in Chiba) of the NIRS (National Institute of Radiological Sciences, Chiba, Japan). Prior to this

work we have shown that the ion-induced degradation of the scintillation intensity can be neglected for fluence lower than 10^{12} ions/cm^2 [11]. We present the dosimeter prototype and its response under ion beam. We show that, when the ion energy is changed, the scintillation, after noise subtraction, gives a Bragg curve-like signal. The choice of scintillator thickness is discussed and it is shown that the scintillation signal is better described by a model taking into account the energy deposited by secondary electrons.

II. Material and methods

A. Dosimeter prototype

We use a polyvinyltoluene based plastic scintillator, BC418 from Bicron, whose density is 1.032 g/cm^3 and main emission wavelength is 360 nm. The scintillator (of 10 mm^2 surface) is inserted inside a 6 mm in diameter measurement probe which consists in a suprasil quartz light guide, coated with Titanium; a mirror at the top of the measurement probe reflects scintillation into the light guide. The probe is directly connected to a 600 µm silica core optical fibre, whose length is 20 m. The output of the fibre is connected to the H7155-20 photon counting unit (Hamamatsu). This device includes a pre-scaler and amplifier so that the output TTL signal can be directly delivered to the M8784 counting board (Hamamatsu). The photon counting unit is biased at 5 V and it can be either operated by selecting a constant integration time or in external trigger mode. The light guide, optical fibre and the photon counting unit are adapted to perform measurements in the UV-ViS spectral range. An overview of the prototype is depicted in **Figure 1.**

B. Irradiation conditions

The prototype has been tested in the "Bio Room" of the HIMAC facility using the following ions: ^{4}He (150 MeV/A), ^{12}C (290 MeV/A) and ^{20}Ne (400 MeV/A). A 10 cm in diameter uniform beam, operated in pulse mode, has been used for all ions. After the beam calibration a depth-dose reference curve is obtained. During the experiment the water equivalent depth is obtained by moving energy degraders (PMMA) of different thickness, located in front of the dosimeter. The dose at a given depth can be calculated using the number of Main Monitor Counts (MMC), as recorded from the upstream main beam monitor, and the depth-dose reference curve obtained during beam calibration. Details on the irradiation system and calibration protocol can be found in [12], all our data are normalized according to the MMC. The depth-dose reference curve for Carbon and Helium ions is given in **Figure 2**, measurements have been carried out for all depth marked by symbols on this curve. For Helium, Carbon and Neon the mean fluences per pulse were respectively 8.10^{4}, 3.10^{5} and 7.10^{4} ions/cm^{2}. The measurement probe is set up in horizontal position, so that the scintillator is located at the centre of the irradiation field, marked by two laser beams. For each point of the reference curve measurements are carried out using between 25 and 50 pulses. The results presented in section III have been obtained operating the photon counting unit in external trigger mode, *i.e.* the H7155-20 integrates the total number of photons during a time gate as large as the ion pulse. When the dosimeter is irradiated without scintillator we obtain a background signal which is measured in the same conditions as described above.

C. Data processing

Off-line processing of the data (background and scintillation signal) is as follow.

(i) Counting linearity correction. As stated by the manufacturer the H7155-20 counts can be corrected knowing the pulse pair resolution (1 ns). Since the measured counts are

far below the non linear range this step could be completely neglected but is performed for completeness.

(ii) Construction of the relative photon counts distribution. For each pulse the number of PhotoMultiplier Counts (PMC) is divided by the MMC and the distribution of this ratio is characterized by its mean and gaussian standard deviation. When the number of pulse is not enough to ensure reliable gaussian fitting the usual mean and standard deviation are used.

(iii) Net signal calculation. The net signal Per (main) Monitor Counts, S_{pmc}, is simply obtained by subtracting the means of the total and background signal.

The uncertainty on S_{pmc} is calculated as follows:

$$\frac{\Delta S_{pmc}}{S_{pmc}} = \sqrt{\left(\frac{\sigma_{Backgorund}}{S_{Background}}\right)^2 + \left(\frac{\sigma_{Total}}{S_{Total}}\right)^2}, \quad (1)$$

where S_{Total} is the scintillation signal per monitor count before subtraction of the background signal.

III. Results and discussion

A. Scintillator thickness and dosimeter gain

In order to describe the dosimeter response we give in **Table 1** the signal gain, defined as the ratio of the maximum signal value to the plateau value, obtained at the highest energy. As illustrated in **Figure 3** the subtraction of the background signal is essential in order to evaluate correctly the gain: after subtraction the maximum of the signal is shifted to larger depth since the ratio of the total signal to the background signal is energy dependant. As expected, the thinner the scintillator the higher the gain, indeed for the energies producing the Bragg peak the scintillator responds to the ion energy rather than to the ion stopping power. Gain variation with scintillator thickness is illustrated in **Figure 4.** Even for the thinnest scintillators that have been used the gain is far below the gain in dose, this is due to the well

known saturation of the scintillation yield with increasing stopping power. As a consequence, for 20 µm scintillators the gain is higher for ions of lower charge. Using 60 MeV protons and equivalent scintillators Torissi [10] has found a gain of 3.2 for a thickness of 500 µm, such a gain is reachable for Helium with a thickness of 10 µm.

From a practical point of view, a low gain is a drawback, but not a crippling problem if the measurements are accurate enough. For Carbon ions the typical uncertainty is of 10% for 10-20 µm, of 7% for 30-50 µm and of 5% for 100-200 µm. For Helium and Neon, under lower fluence, the respective typical uncertainties are 12% and 7%.

B. Scintillation variation with stopping power

Several models have been proposed in order to describe the velocity effect and the saturation mechanism which are the two main features of ion-induced scintillation. In the pioneer work of Birks [13], the specific scintillation per ion, S_{PI}, is given as a function of the stopping power:

$$\frac{dS_{PI}}{dx} = A\frac{dE/dx}{1+k_B.(dE/dx)}, \qquad (2)$$

where k_B is generally called the quenching parameter. Even if this model is useful to describe the scintillation induced by one kind of ion it is known that the quenching parameter is in fact ion dependant. Indeed, if we attempt to describe the experimental scintillation per ion, using the data obtained with 20 µm scintillator, we find for k_B the values given in **Table 2.** The value obtained for Helium is in agreement with the values given in [10] for 60 MeV protons, but for Helium and Neon the k_B value is one order of magnitude smaller.

In order to describe the ion induced scintillation with parameters independent of the ion charge, the BVT model, introduced by Tarlé [14] and Ahlen [15], following the work of Voltz

et al. [16], suggests introducing the quenching of ionisation energy in the core of the ion track; the specific scintillation is then:

$$\frac{dS_{PI}}{dx} = C\frac{dE}{dx}\left\{F_s + \frac{1-F_s}{1+B_s(1-F_s)dE/dx}\right\} \tag{3}$$

The fraction of the total energy loss, giving raise to scintillation in the halo is F_s, given by:

$$F_s = \frac{1}{2}\frac{\ln(2mc^2\beta^2\gamma^2/T_0)-\beta^2}{\ln(2mc^2\beta^2\gamma^2/I_{adj})-\beta^2}. \tag{4}$$

The usual Lorentz parameter are β and γ, m is the electron mass, I_{adj} = 64.7 eV is the adjusted ionisation potential for vinyltoluene plastic scintillator and T_0 is a free parameter, such that delta rays of energy greater than T_0 escape the track core. In the track core a quenching, linear with stopping power, with efficiency B_s, is assumed. Applying this model we find the best adjustment for B_s=5.10^{-2} µm/keV and T_0=9.7 keV. This values can be compared with T_0=11.5 keV and B_s=10^{-1} µm/keV, found in [15], for heavy ions irradiating the scintillator Pilot-Y. In this model the spreading of the normalisation constants, C, used for each ion is not too large, as show in the inset of **Figure 5**, but the quality of the fit is far from being satisfying.

Michaelian and Menchaca-Rocha [17-18] have also proposed a universal model for ion induced scintillation in organic and inorganic scintillators (MM model). They consider an ion track core where the scintillation cross section is constant and a halo where the scintillation is proportional to the total radial dose, $\rho(r)$. Calling dNe/dx the linear density of charge carrier we have:

$$\frac{dN_e}{dx} = \pi r_q^2\rho_q + \int_{r_q}^{R_{\max}}\rho(r)2\pi r dr, \tag{5}$$

and

$$\frac{dS_{PI}}{dx} = C\frac{dN_e}{dx}\left\{1 - F\frac{dNe/dx}{A+dNe/dx}\right\}. \tag{6}$$

The quenching density, ρ_q, is a free parameter, defined so that the core is the region where the radial dose is superior to ρ_q. The maximum range of secondary electrons is R_{max} and r_q is the radius at which the radial dose equals the quenching density. The inefficiency for production of luminescence through bimolecular process is given by F and A is the number of entities in the material which allow a triplet state to transform into a singlet. Like in **Eq. (3)** an overall normalisation constant, C, is used; this normalisation constant is supposed to be the same for all ions but in the fitting procedure a constant is found for each ion and the spreading of these constants is examined. In all the calculation we use the radial dose expression given in [17]. Applying this more complex model, we find the best adjustment for ρ_q=1250 erg/g =0.125 Gy, F=0.9, and A=1.1 10^{-4}. The quality of the fit is much better than that obtained using **Eq. (3)**, as shown in **Figure 5** and **Table 2**. The value of A is close to the value given in [19] for plastic scintillators and the value of the quenching density is difficult to compare with other values, because it has been found in the order of 10^6 erg/g in [18], and between 10^2 and 10^{-3} erg/g in [19].

C. Cross calibration

Since the models describing ion-induced scintillation are established using the ion energy or stopping power as input data and since the dose delivered by the ion beam includes several nuclear fragments of different velocities, especially near the stopping point, it is useful to establish a relation between S_{pmc} and the relative dose, given during the calibration of the beam. In **Figure 6** we report S_{pmc} as a function of the dose per main monitor counts, as it can be seen a linear relation can be established between S_{pmc} and the relative dose, for convenience the data shown in **Figure 6** are normalized, so that S_{pmc} measured at the nominal energy is set equal to the relative dose at this energy. The linear relationship is valid up to the maximum dose found in the Bragg peak.

IV. Conclusion and outlook

Despite the saturation of scintillation efficiency with increasing power we have shown that it is possible to obtain Bragg curve-like signal using thin plastic scintillator as dose convertor. The use of thinner scintillator thickness could lead to higher gain but with the current design of this prototype the accuracy of measurement would be limited due to the low count rate. Better accuracy in the measurement could be obtained by improving the light collection efficiency, particularly if the optical fibre length was decreased. The use of a second measurement channel, without scintillator, to directly perform the background signal subtraction, should also improve the accuracy of measurements.

Acknowledgments

This experiment (16P168) was performed as part of the Research Project with Heavy Ions at NIRS-HIMAC. We would like to express our thanks to the staff of HIMAC. We would like also to thank the Japanese Society for the Promotion of Sciences and French government for supporting this work in the framework of the Sakura Japan France Joint Research Program, (contract 06871 UL).

References

[1] A Fukumura, T Hiraoka, K Omata, M Takeshita, K Kawachi, T Kanai, N Matsufuji, H Tomura, Y Futami, Y Kaizuka and G H Hartmann, Phys. Med. Biol., 44 (1998) 12.

[2] M. Durante, G. F. Grossi, M. Pugliese, and G. Gialanella, Radiat. Meas., 26 (1996) 2.

[3] R. Bonin, A. Boriano, F. Bourhaleb, R. Cirio, M. Donetti, E. Garelli, S. Giordanengo, F. Marchetto, C. Peroni, C. J. Sanz Freire, and L. Simonetti, Nucl. Instr. and Meth. A, 519 (2004) 3.

[4] H. J. Brede, O. Hecker, and R. Hollnagel, , Nucl. Instr. and Meth. A, 455 (2000) 3.

[5] A.S. Beddar, K.J. Kinsella, A. Ikhlef, and C.H. Sibata, IEEE. Trans. Nucl. Sci. 48 (2001) 3.

[6] A.S. Beddar, S. Law, N. Suchowerska, and T. R. Mackie, Phys. Med. Biol. 48 (2003) 9.

[7] J.M. Fontbonne, G. Iltis, G. Ban, A. Battala, J.C. Vernhes, J. Tillier, N. Bellaize, C. Le Brun, B. Tamain, K. Mercier, and J.C. Motin, IEEE. Trans. Nucl. Sci. 49 (2002) 5.

[8] F. Pain, P. Laniece, R. Mastrippolito, Y. Charon, D. Comar, V. Leviel, J.F. Pujol, and L. Valentin, IEEE. Trans. Nucl. Sci. 47 (2000) 1.

[9] F. Pain, P. Laniece, R. Mastrippolito, L. Pinot, Y. Charon, A. Glatigny, M.T. Guillemin, P. Hantraye, V. Leviel, L. Menard, and L. Valentin, IEEE. Trans. Nucl. Sci. 49 (2002) 3.

[10] L. Torrisi, Nucl. Instr. and Meth. B 170 (2000), 3-4.

[11] D. Broggio, J.M. Jung, R. Barillon, and T. Yamauchi, Radiat. Meas. 40 (2005) 2-6.

[12] T. Kanai, M. Endo, S. Minohara, N. Miyahara, H. Koyama-Ito, H. Tomura, N. Matsufuji, Y. Futami, A. Fukumura, T. Hiraoka, Y. Furusawa, K. Ando, M. Suzuki, F. Soga, and K. Kawachi, Int. J. Radiat. Oncol. Biol. Phys. 44 (1999) 1.

[13] J. B. Birks, Phys. Rev. 54 (1951) 2.

[14] G. Tarlé, S. P. Ahlen, and B. G. Cartwright, Ap. J. 230 (1979).

[15] M. Salamon and S.P. Ahlen, Nucl. Instr. and Meth. A 195 (1982) 3.

[16] R. Voltz, J. Lopes da Silva, G. Laustriat, and A. Coche, "*Influence of the Nature of Ionizing Particles on the Specific Luminescence of Organic Scintillators*", J. Chem. Phys., vol. 45, no. 9, pp. 3306-3311, Nov. 1966.

[17] K. Michaelian and A. Menchaca-Rocha, Phys. Rev. B 49 (1994) 22.

[18] K. Michaelian, A. Menchaca-Rocha, and E. Belmont-Moreno, Nucl. Instr. and Meth. A 356 (1995) 2-3.

[19] A. Menchaca-Rocha, M. Buénerd, L. Gallin-Martel, F. Ohlsson-Malek and T. Thuillier, Nucl. Instr. and Meth. A 438 (1999), 2-3.

Table caption

Table 1.
Dosimeter gain for different scintillator thickness.

Table 2.
Fit parameters used to describe ion-induced scintillation.

Figure caption

Figure 1. Dosimeter overview. The photos at the bottom show details of the measurement probe with inserted scintillators and of the fiber optic connection to the photon counting unit.

Figure 2. Reference curve of the dose per Main Monitor Counts for Helium ions (square) and Carbon (triangle). Measurements have been carried out at the marked points, line are drawn to guide the eye.

Figure 3. Effect of background subtraction: Neon and 40 µm scintillator (top curves), Helium and 20 µm scintillator (bottom curves). The scintillation signal per monitor counts (full line) is obtained by subtracting the total signal (dash dotted line) and the background signal (dotted line). The small graphs on the right represent the zoom of the large plots around the Bragg peak.

Figure 4. Illustration of the variation of dosimeter gain with scintillator thickness for carbon ions: 20 µm (a), 30 µm (b) and 100 µm (c). The scintillation per monitor counts is normalized to 1 at nominal energy and the lines are drawn to guide the eye.

Figure 5. Scintillation per ion as a function of stopping power fitted with the BVT model (dotted line) and with the model of Michaelian and Menchaca-Rocha (full line). Helium data are marked with squares, Carbon with triangles and Neon with circles. The inset shows variation of normalisation constants according to Z for the studied ions: BVT model (*) and MM model (+).

Figure 6. Linear relation between the scintillation signal per monitor counts and the relative dose. Top curve is for Helium ions and 20 µm scintillator. Bottom curve is for Carbon ions and 30 µm scintillator (triangles), Neon ions and 40 µm scintillator (circles). The data are normalized so that the scintillation signal equals the relative dose at nominal energy.

Figure 1

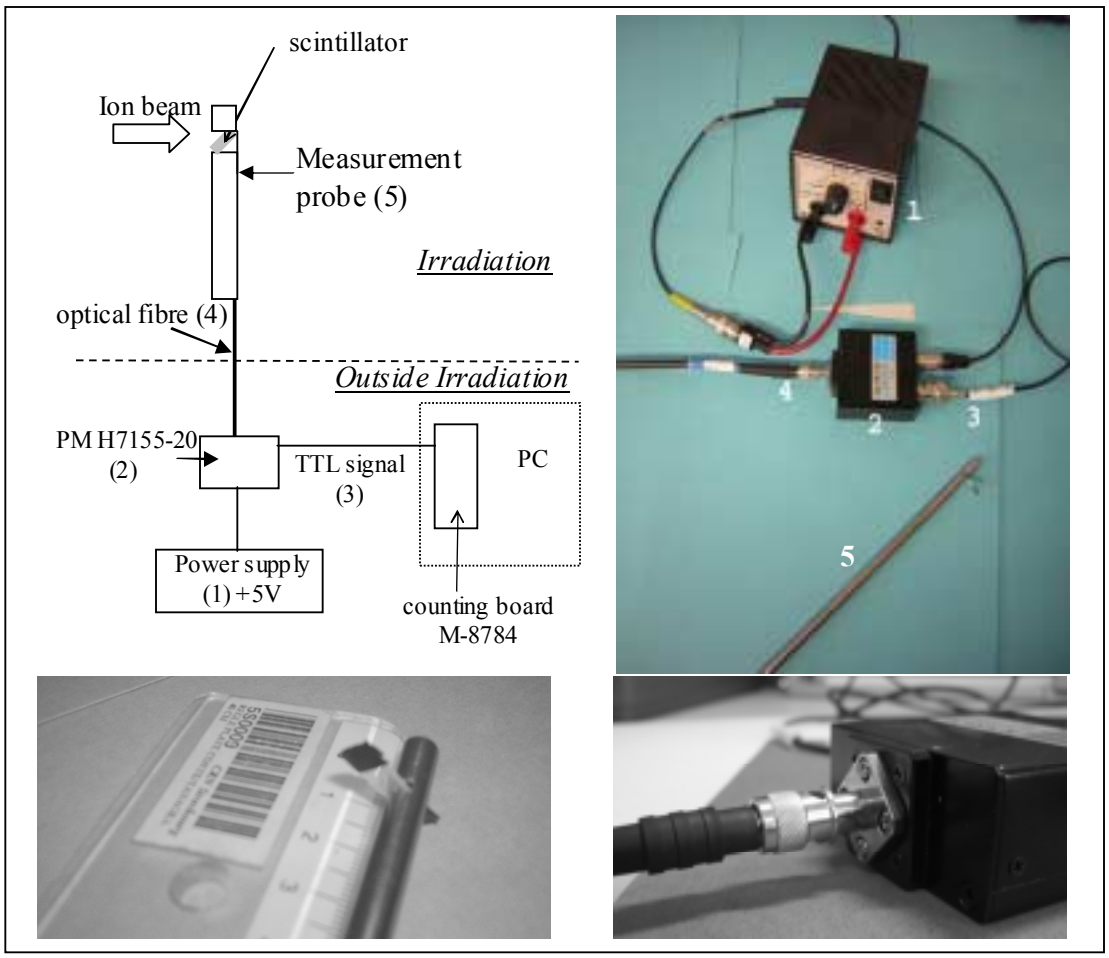

Polyvinyltoluene scintillators for relative ion dosimetry: an investigation with Helium, Carbon and Neon beams.
David Broggio et al.

Figure 2

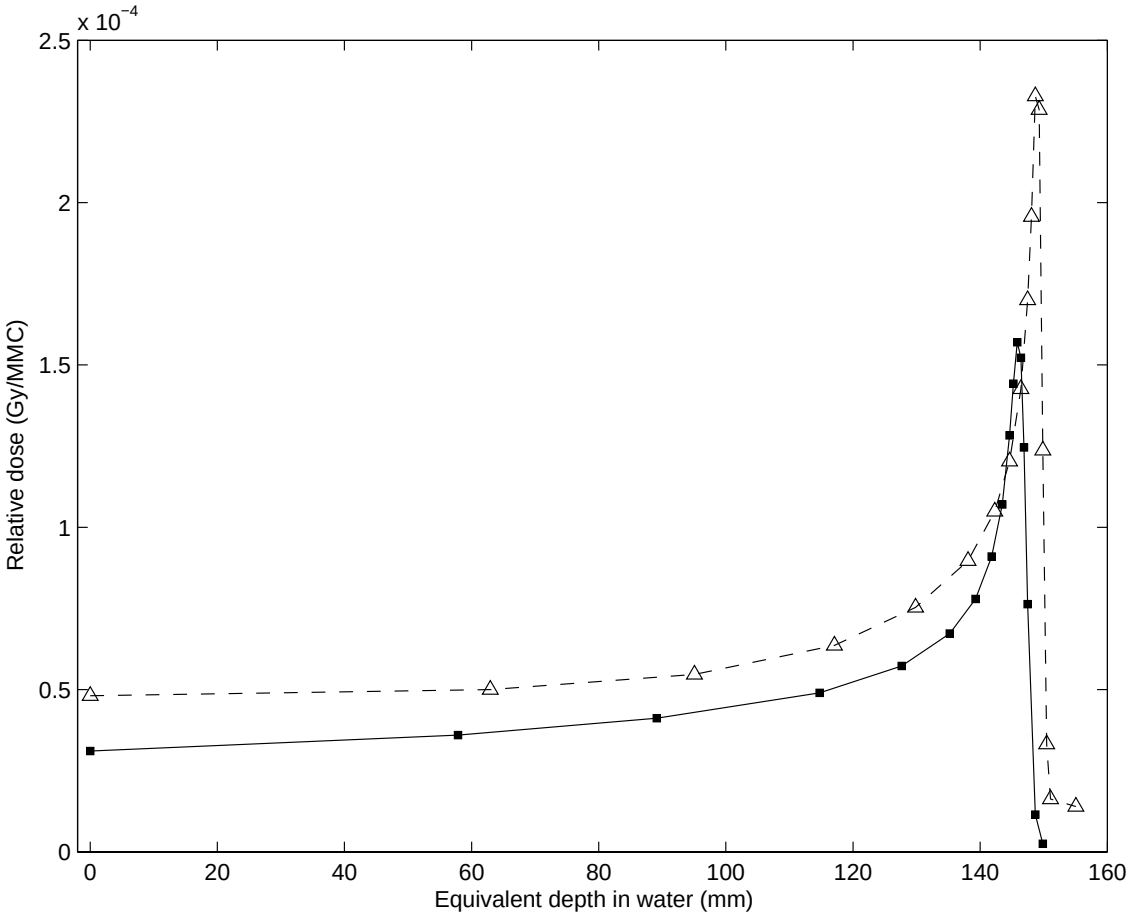

Polyvinyltoluene scintillators for relative ion dosimetry: an investigation with Helium, Carbon and Neon beams.
David Broggio et al.

Figure 3

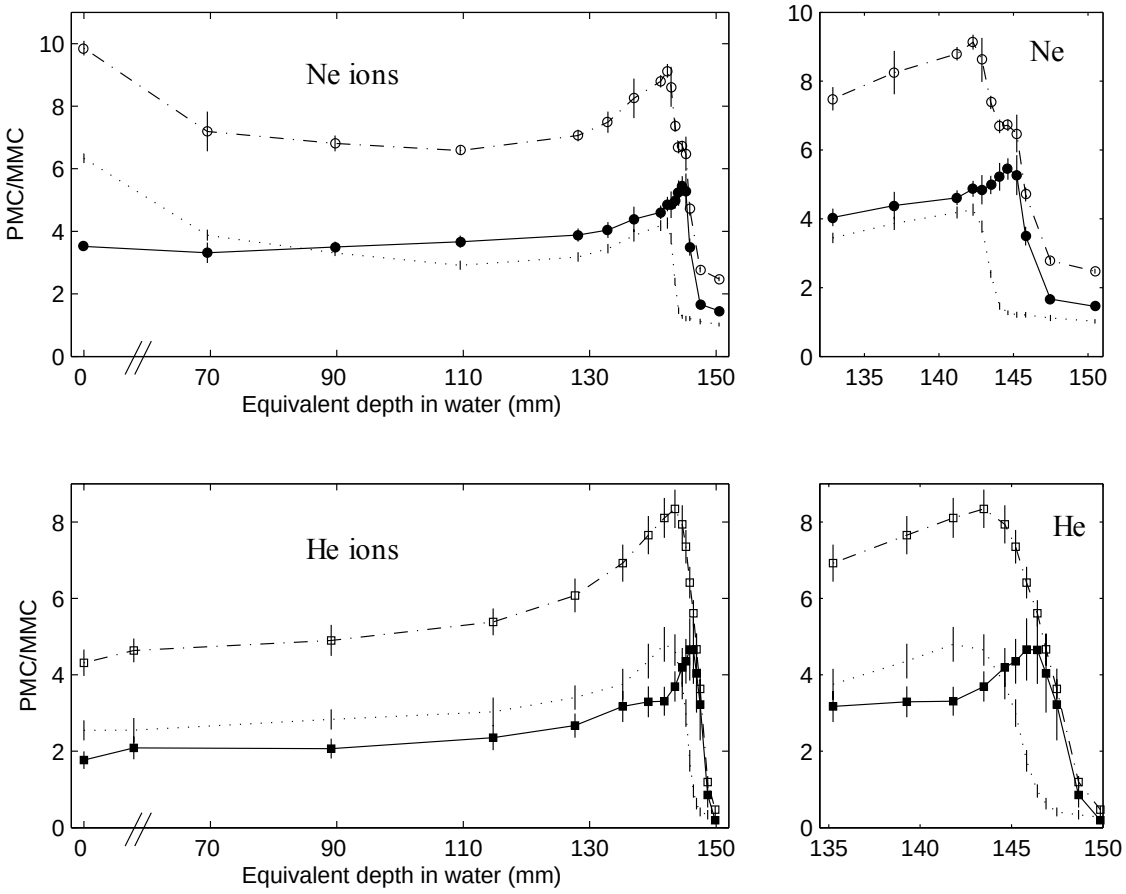

Polyvinyltoluene scintillators for relative ion dosimetry: an investigation with Helium, Carbon and Neon beams.
David Broggio et al.

Figure 4

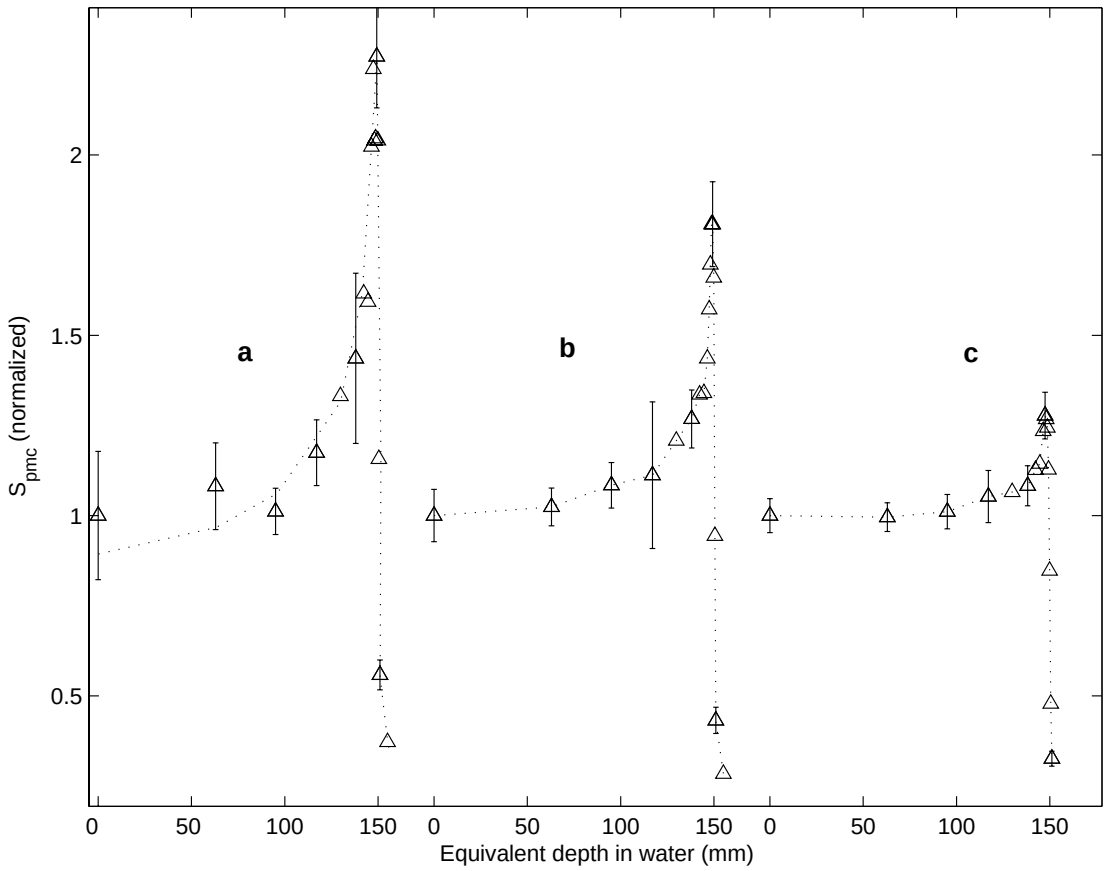
a
b
c
S_{pmc} (normalized)
Equivalent depth in water (mm)
0.5
1
1.5
2
0
50
100
150

Figure 5

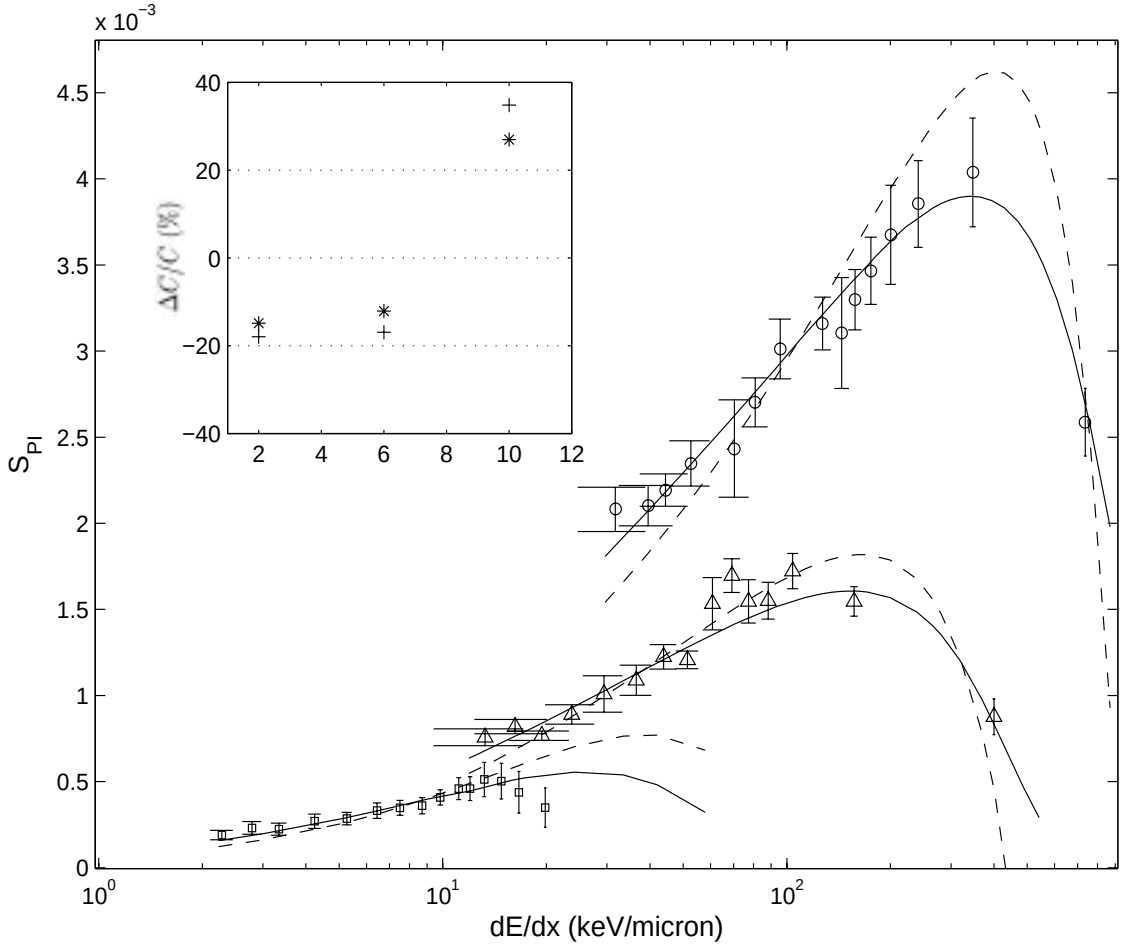
x 10^-3
4.5
4
3.5
3
2.5
2
1.5
1
0.5
0
S_PI
10^0
10^1
10^2
dE/dx (keV/micron)
40
20
0
−20
−40
ΔC/C (%)
2
4
6
8
10
12

Figure 6

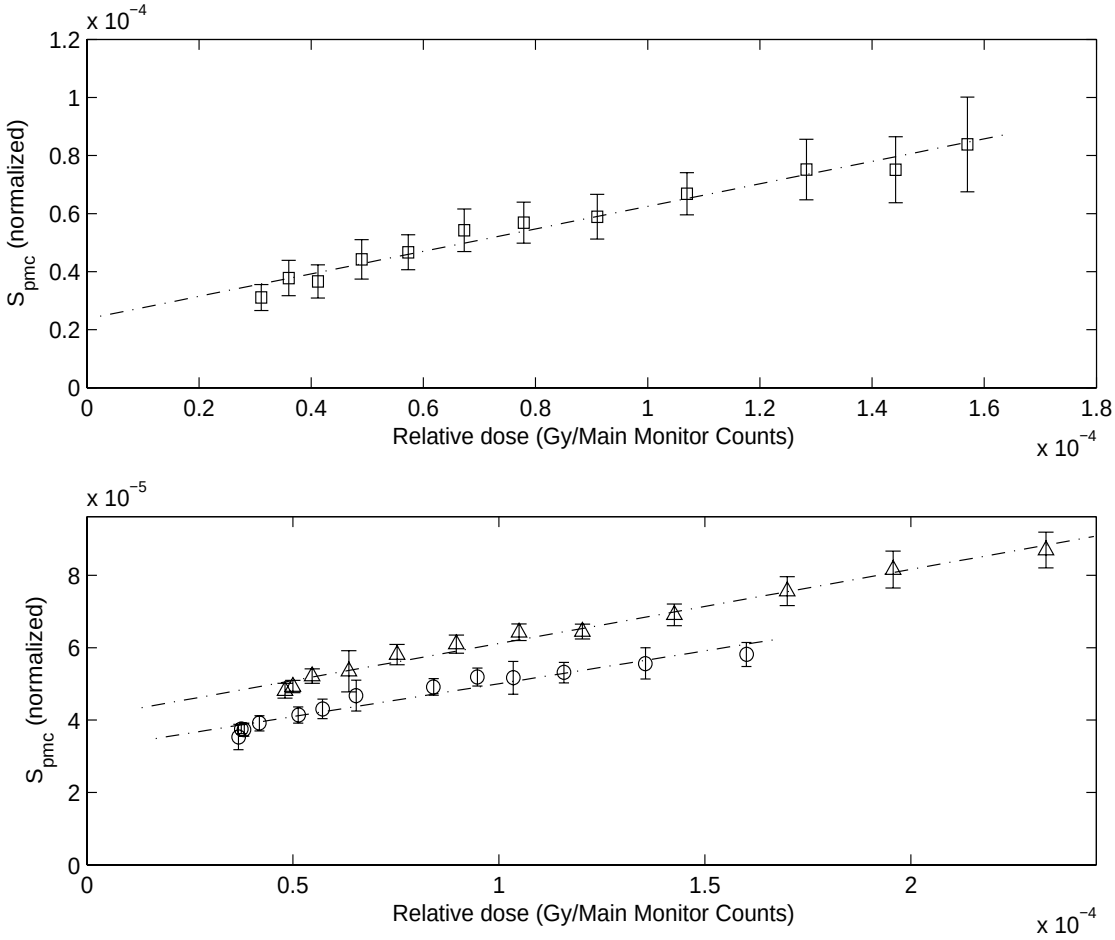
x 10^-4
1.2
1
0.8
0.6
0.4
0.2
0
S_pmc (normalized)
0
0.2
0.4
0.6
0.8
1
1.2
1.4
1.6
1.8
Relative dose (Gy/Main Monitor Counts)
x 10^-4
x 10^-5
8
6
4
2
0
S_pmc (normalized)
0
0.5
1
1.5
2
Relative dose (Gy/Main Monitor Counts)
x 10^-4

Table 1.

Ion	Helium			Carbon				Neon		
Scintillator thickness (μm)	10	20	40	20	30	50	100	10	20	40
Dosimeter gain	3.3 ±1	2.7±0.9	2.5±0.7	2.1±0.5	1.8±0.3	1.8±0.3	1.3±0.1	2.9±0.4	1.9±0.3	1.5±0.1

Table 2.

Birks	BVT	MM
kB = 0.16 µm/keV (Helium)	$B_s = 5.10^{-2}$ µm/keV	ρ_q = 0.125 Gy
kB = 0.04 µm/keV (Carbon)	T_0 = 9.7 keV	F = 0.9
kB = 0.02 µm/keV (Neon)	χ^2/n = 3.07	A = 1.1 10^{-4}
		χ^2/n = 1.03